INTERNATIONAL ATOMIC ENERGY AGENCY
UNITED NATIONS EDUCATIONAL, SCIENTIFIC AND CULTURAL ORGANIZATION
INTERNATIONAL CENTRE FOR THEORETICAL PHYSICS
I.C.T.P., P.O. BOX 586, 34100 TRIESTE, ITALY, CABLE: **CENTRATOM TRIESTE**

H4.SMR/638-19

College on Medical Physics:
Imaging and Radiation Protection

31 August - 18 September 1992

Methods for Producing Biomedical Images through the Reconstruction from Projections

E. Staderini

Università degli Studi
"La Sapienza"
Centro per Ingegneria Biomedica
Rome, Italy

METHODS FOR PRODUCING BIOMEDICAL IMAGES THROUGH THE RECONSTRUCTION FROM PROJECTIONS

Dr. Enrico M. Staderini

The physics and technology of computed tomography (CT) applications are summarized in Table I (modified from [1]). The emanations (i.e. the sources of energy) used to test the object are listed in that table along with the measured physical quantities and the transducers most usefully employed.

This is to remind both to the large number of technological possibilities available nowadays for performing a computed tomography, and the vast application field for the various methods of image reconstruction from projections.

Most used emanations are X-rays, acoustic waves, magnetic and radio-frequency electro-magnetic fields, which have permitted the carrying out of practical systems for CT, echography and NMR (nuclear magnetic resonance) tomography.

TABLE I: PHYSICS AND TECHNOLOGY OF CT APPLICATIONS

Emanations used	Densities measured	Transducers employed	Applications
X-rays	attenuation coefficients	X-ray sources scintillation detectors	Diagnostic Radiology (DR) Nondestructive Testing (NDT)
Gamma-rays	concentration of radio-labeled substance	scintillation counters	DR, Nuclear Medicine
Compton scattered X-rays, Gamma-rays	electron density or distribution of atomic number	X-ray sources scintillation counters	DR, NDT X-ray crystallography
Heavy particles	scattering/absorbtion cross section	linear accelerators stacked detectors	DR,NDT
Electron beams	Schrodinger potential distribution	electron guns, film photomultiplier/TV	Microscopy
Acoustic waves	attenuation refractive index acoustic impedance	electro-mechanical devices	DR, NDT Geological Prospecting (GP)
Low-frequency electric currents	electr. conductivity distribution	electrodes	Imaging of blood vessels GP, NDT
Magnetic fields	distribution of nuclear spins blood flow	magnets, RF coils magnetometers	Nuclear Magnetic Resonance (NMR) Magneto-Hydro-Dynamic (MHD)
Radio-frequency fields	electron spins permittivity and conductivity distribution	capacitors, coils antennas, horns	NMR, Mapping
Spatially incoherent electromagnetic radiations	volume temperature distributions celestial brightness distributions	horns, antennas telescopes	Mapping temperature distrib. Astronomical imaging

As far as the control extension on the sources employed is concerned, three main tomography techniques may be defined.

When the sources are emitting from inside the body, the experimenter can do nothing over them but remotely sense their emanations coming from the body. This operation is called remote sensing computed tomography (Table II).

Another aspect of computed tomography concerns the use of sources applied externally of the body and measuring the emanations passed through the object. This is the remote probing computed tomography (Table III).

In combined probing-sensing computed tomography, we deal with emanations generated from sources placed inside the body after a sort of stimulation or excitation derived from external emanations (Table IV).

TECHNIQUES APPLIED FOR REMOTE-SENSING CT
Single Photon Emission Computed Tomography (SPECT)
Positron Emission Tomography (PET)
Super Synthesis (e.g. Earth rotation synthesis telescope)

TABLE II

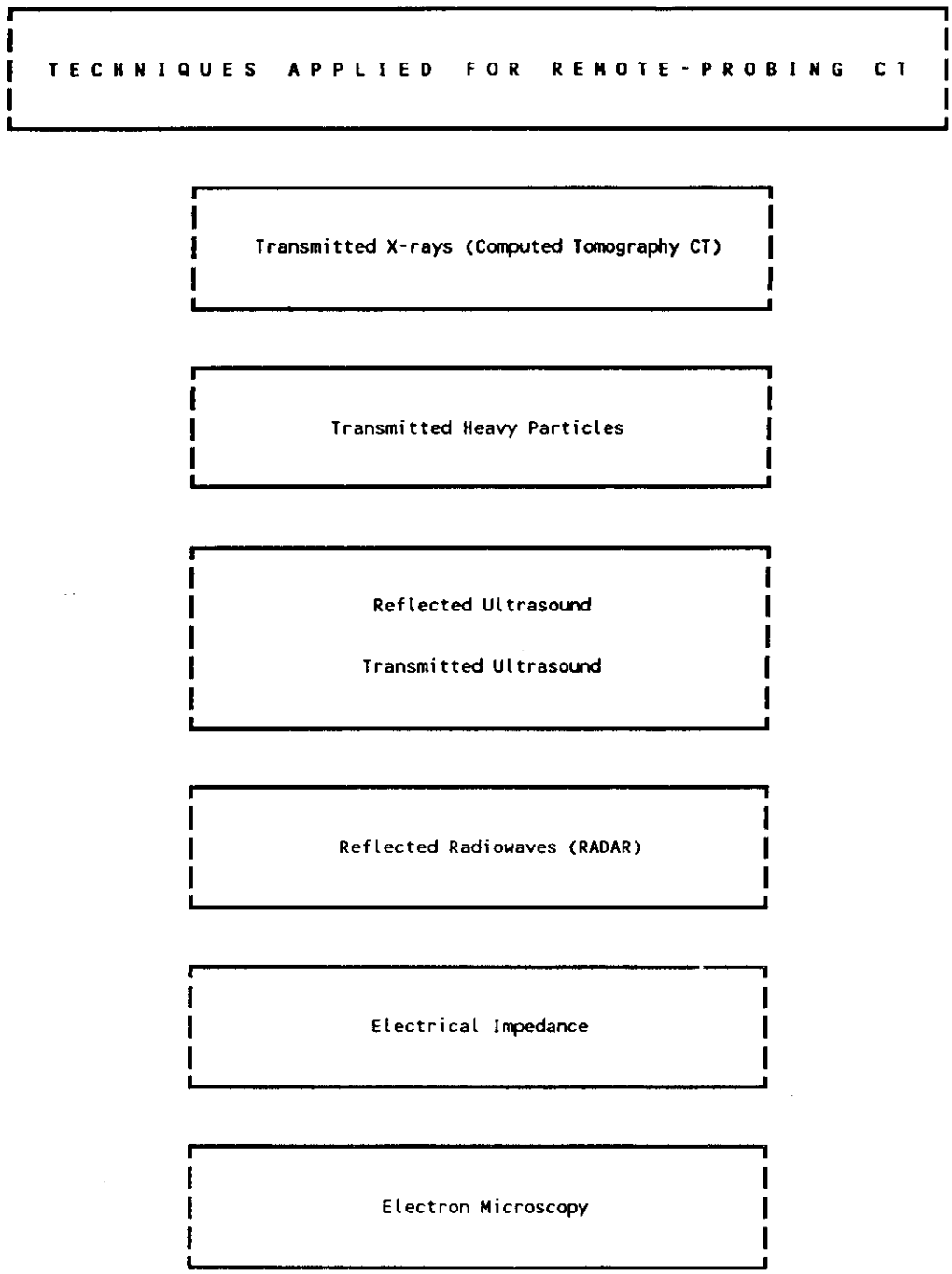
TECHNIQUES APPLIED FOR REMOTE-PROBING CT
Transmitted X-rays (Computed Tomography CT)
Transmitted Heavy Particles
Reflected Ultrasound
Transmitted Ultrasound
Reflected Radiowaves (RADAR)
Electrical Impedance
Electron Microscopy

TABLE III

TECHNIQUES APPLIED FOR PROBING-SENSING CT
Nuclear Magnetic Resonance (NMR)
Corrected Emission
Uncorrected Compton Scatter
Corrected Compton Scatter
Magneto-Hydro-Dynamic

TABLE IV

GEOMETRICAL PRELIMINARIES

First of all let us consider the projection ray geometry. In fig. 1 a circular body, the attenuation coefficient of which has to be measured on section z, is passed through by a ray having an angle ϑ and a displacement s respect to the center of the body coordinates.

In the body z plane the coordinates (x,y) of the point P may be expressed in terms of s and ϑ as:

$$x = R \cos\phi = s \cos\vartheta - t \sin\vartheta \qquad [1]$$

$$y = R \sin\phi = s \sin\vartheta + t \cos\vartheta \qquad [2]$$

The inverse relation also holds:

$$s = x \cos\vartheta + y \sin\vartheta \qquad [3]$$

$$t = y \cos\vartheta - x \sin\vartheta \qquad [4]$$

The problem of tomographic reconstruction from projections is simply to find the function [5], in the section plane x,y at z, giving the distribution of the physical variable to be estimated:

$$V = f (x , y) \qquad [5]$$

given the set of projections for each angle ϑ and displacement s:

$$p (s , \vartheta) = \int_{-T}^{T} f (s \cos\vartheta - t \sin\vartheta , s \sin\vartheta + t \cos\vartheta) \, dt \qquad [6]$$

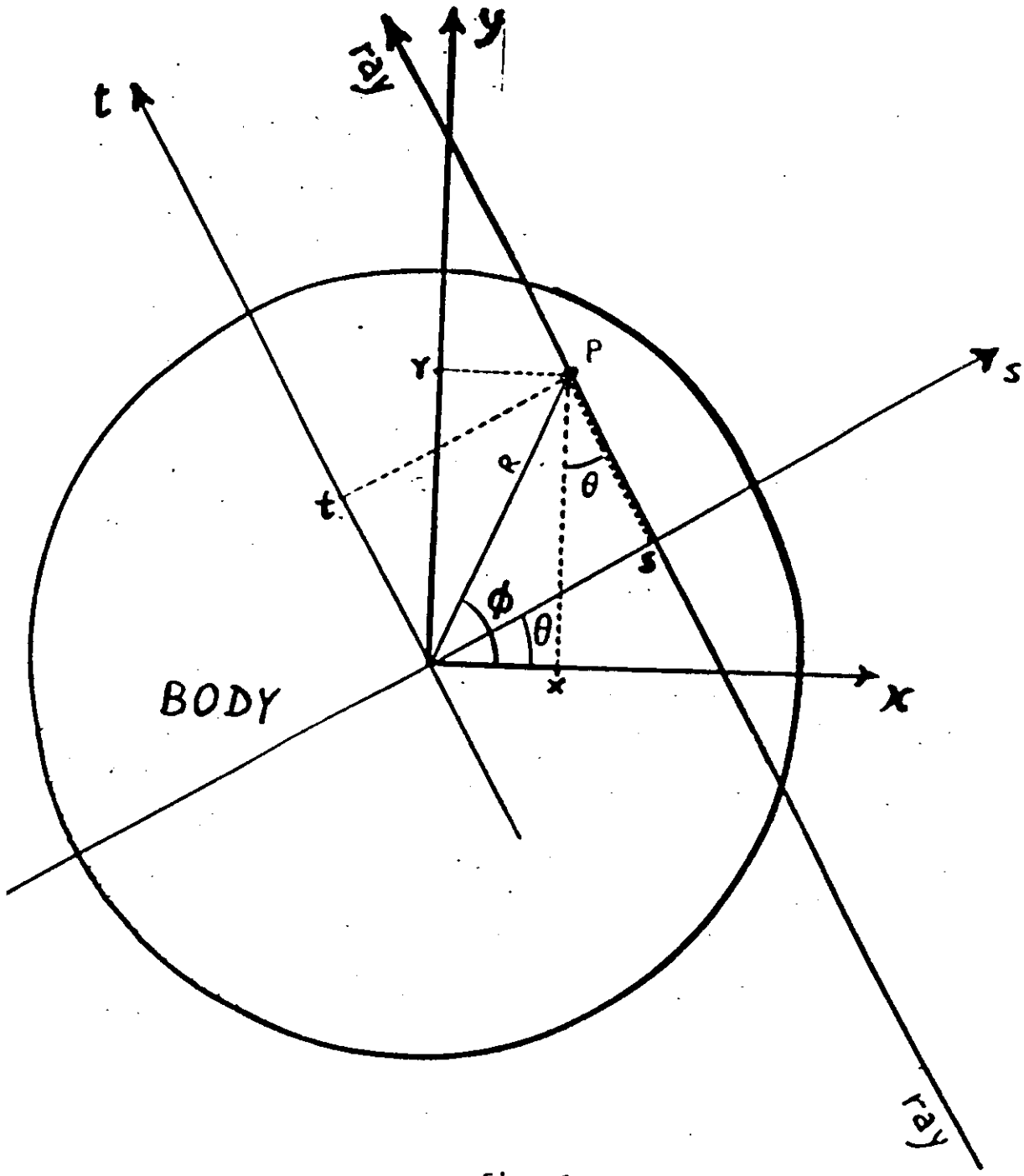

fig. 1

where $T(s) = (1 - s^2)^{1/2}$ $\quad |s| \leq 1$ [7]

and $p(s, \theta) = 0$ $\quad |s| > 1$ [8]

Please note that we are not in the presence of a polar coordinate system as:

$$p(0, \theta_1) = p(0, \theta_2) \quad [9]$$

Note also the periodism:

$$p(s, \theta) = p(-s, \theta + \pi) \quad [10]$$

INTERACTION WITH MATTER

Figure 2 shows the effect of linear attenuation of a beam of intensity I_o when passing through an absorbing medium. The linear attenuation coefficient μ is a function of the energy of the photons and of the atomic number and density of the matter. If the specimen is not homogeneous, then μ is also a function of the spatial coordinates. Moreover, if the beam is polychromatic, only a mean of μ over present energies can be measured.

At the bottom of fig. 2 the experimental projection function is determined as a function of the measured quantities.

$$\frac{dI}{dx} = -\mu_t I \qquad I = I_0 e^{-\mu_t x}$$

$$\mu = f(E, Z, \rho, \text{polariz.}, x, y)$$

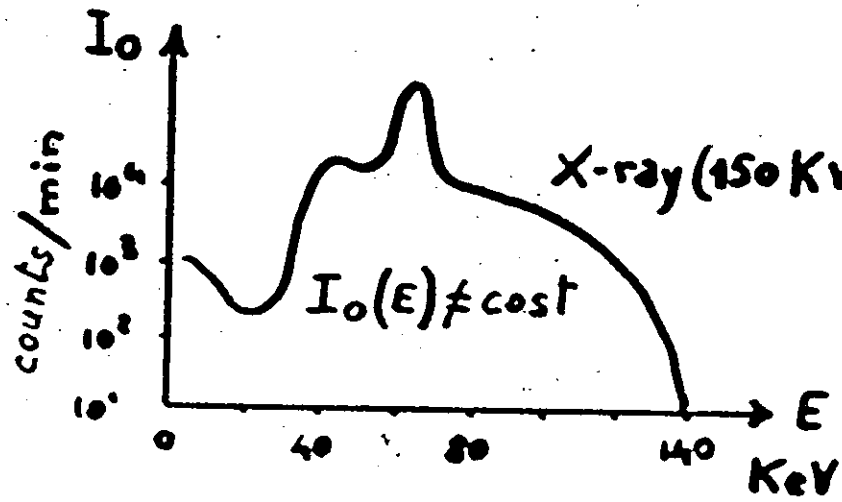

$$I(s,\theta) = I_0 e^{-\int_{s,\theta} \mu(x,y)\,dt}$$

$$p(s,\theta) = \ln\left(\frac{I_0}{I(s,\theta)}\right)$$

fig. 2

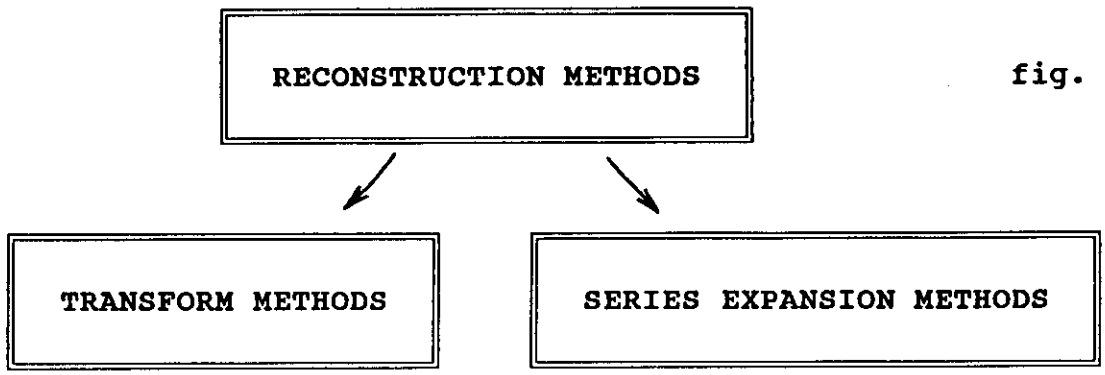

fig. 3

TRANSFORM METHODS

In the transform methods the problem of reconstruction from projections is faced by formulating a mathematical model in which known and unknown quantities are functions, the arguments of which come from a continuum of real numbers. Then solving for the unknown function with an inversion formula and adapting this formula for discrete or noisy data [2].

The generalized projection theorem is the basis for understanding the two most important transform methods of reconstruction. For any given angle θ the following relation holds:

$$\int_{-1}^{1} P(s,\theta)\, w(s)\, ds = \iint_{\Omega} f(x,y)\, w(x\cos\theta + y\sin\theta)\, dx\, dy \qquad [11]$$

The proof is simply obtained by substituting the left side using [6] and then converting from rotated coordinates using [3] and [4].

An obvious application of this theorem is obtained by using exp ($-i2\pi Rs$) as w(s). In this case it will follow that the 1-D Fourier transform of the projection at angle θ is equal to the

central slice, at the same angle, of the 2-D Fourier transform of the resulting image. This theorem is often known as the projection-slice theorem or the central-section theorem and it allows the practical reconstruction algorithm using the Fourier transform.

Now let us consider the last theorem which can be stated in the following way:

$$\hat{p}\,(R,\theta) = \hat{f}\,(R\cos\theta, R\sin\theta) \qquad [12]$$

It is the central-section theorem where $\hat{p}\,(R,\theta)$ is the 1-D Fourier transform of the projection $p\,(s,\theta)$ with respect to the first variable.

Taking the inverse Fourier transform of [12] we obtain:

$$f(x,y) = \int_0^{\pi}\int_{-\infty}^{\infty} \hat{p}(R,\theta)\, e^{i2\pi R(x\cos\theta + y\sin\theta)}\, |R|\, dR\, d\theta \qquad [13]$$

As the following identity holds:

$$\hat{p}\,(R,\theta_m) = \int_{-1}^{1} p(s,\theta_m)\, e^{-i2\pi Rs}\, ds \qquad [14]$$

for the projection angle θ_m, and considering that we have to deal with sampled data (i.e. we have to use a window function W (R) in order to obtain a band limited reconstructed image f_B (x,y) we have:

$$f_B(x,y) = \int_0^{\pi}\int_{-\frac{1}{2}\Delta s}^{\frac{1}{2}\Delta s} \hat{p}\,(R,\theta)\, w(R)\, e^{i2\pi R(x\cos\theta + y\sin\theta)}\, |R|\, dR\, d\theta \qquad [15]$$

Using [14] we obtain:

$$f_B(x,y) = \int_0^{\pi} \int_{-\frac{1}{2}\Delta s}^{\frac{1}{2}\Delta s} \int_{-1}^{1} p(s,\theta) e^{-i2\pi R s} w(R) e^{i2\pi R(x\cos\theta + y\sin\theta)} |R| \, ds \, dR \, d\theta \quad [16]$$

now considering the following functions:

$$q(s) = \int_{-\frac{1}{2}\Delta s}^{\frac{1}{2}\Delta s} |R| w(R) e^{i2\pi R s} dR \quad [17]$$

$$\hat{q}(R) = |R| w(R) \quad [18]$$

we have:

$$f_B(x,y) = \int_0^{\pi} \int_{-1}^{1} p(s,\theta) q(x\cos\theta + y\sin\theta - s) \, ds \, d\theta \quad [19]$$

after having interchanged the order of integration over s and R.

Note now that the problem of reconstructing the function f_B (x,y) may be split into two parts.

First we can integrate over s and then integrate over θ.

We obtain:

$$\tilde{p}(s',\theta) = \int_{-1}^{1} p(s,\theta) q(s'-s) \, ds \quad [20]$$

which is mathematically a convolution of p (s , θ) using the function q as the convolution kernel.

Then we have:

$$f_B(x,y) = \int_0^{\pi} \tilde{p}(x\cos\theta + y\sin\theta, \theta) \, d\theta \quad [21]$$

in which the parameters of the function p are nothing but the parameters of a ray passing through the point (x,y) at angle θ. The [21] is simply the backprojection of all convolved projections.

The method so described is the well-known filtered back-

projection (as the convolution is nothing but a filter) or convolution back-projection method.

The errors arising from the reconstruction methods are mainly due to technological limitations. These come from:

a) insufficient sampling of the projection

b) errors in estimation of $\hat{p}$

c) errors in the Fourier domain (interpolation, sampling).

As regards the comparation between the Fourier reconstruction and the convolution back-projection one, it has to be stressed that the latter has a far better performance. The Fourier reconstruction algorithm has its weakness in the inelegant 2-D interpolation required, producing images of bad quality. On the other hand, the Fourier algorithm has the potentiality of being performed with less computational effort in respect to the convolution back-projection and this makes the Fourier algorithm worth of being investigated more in detail.

FINITE SERIES-EXPANSION METHODS

In this family of reconstruction methods we are formulating a model which relates a finite set of known numbers with a finite set of unknown numbers. The resulting system of equations is then solved in a numeric way.

The line integral of the unknown attenuation function along the path of the ray can be expressed as in fig. 4, where it is the sum of the products of the attenuation coefficient of each

pixel multiplied by the length of the intersection of the ray i with the squared pixel j.

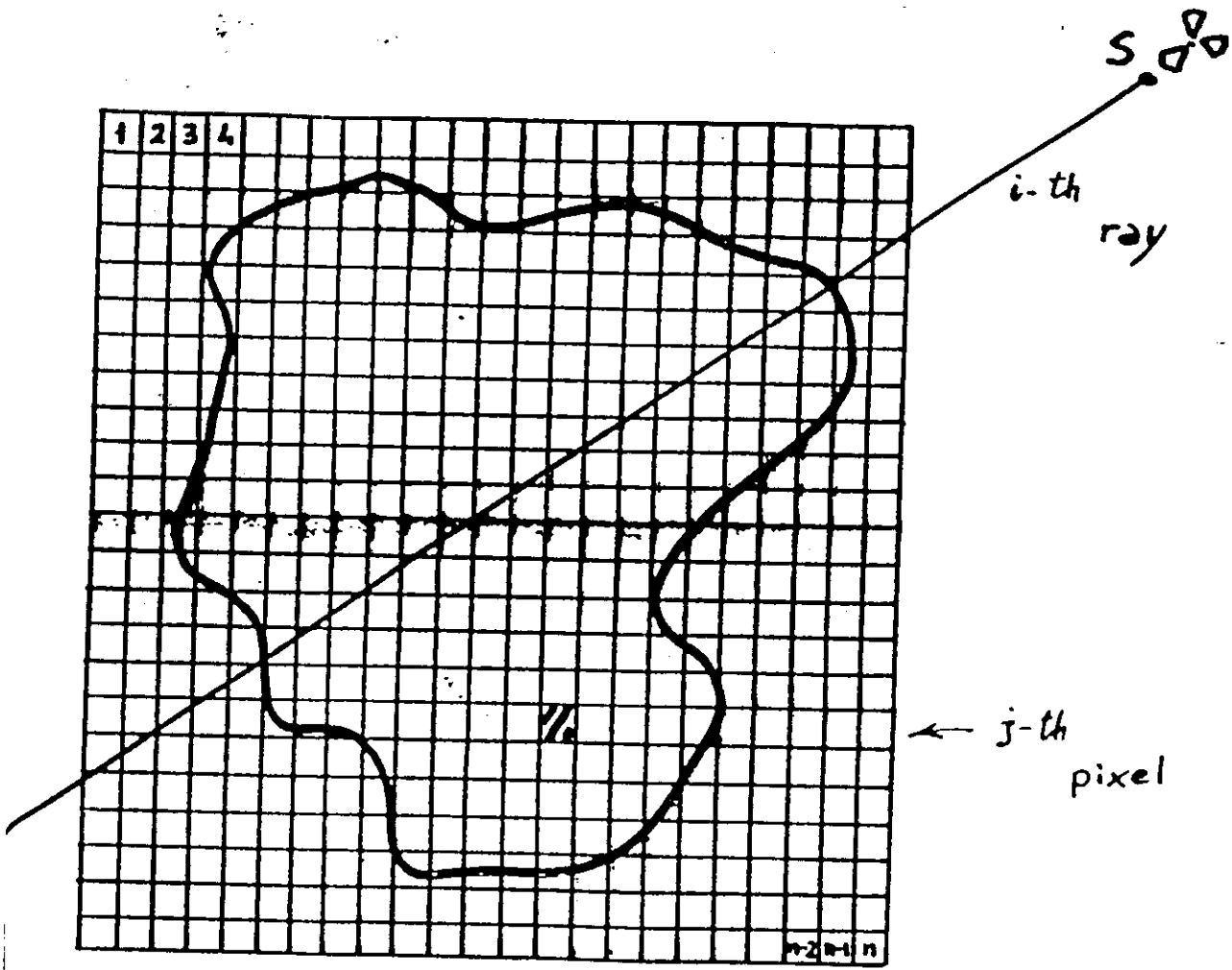

$$\sum_{j=1}^{n} x_j a_{ij} \simeq y_i \qquad i = 1 \cdots m$$

fig. 4

In other words let us consider a set of basis functions in polar coordinates in plane:

$$\left\{ b_j(r,\phi) \right\}_{j=1}^{n} \qquad [22]$$

where

$$b_j(r,\phi) = \begin{cases} 1 & (r,\phi) \in \text{pixel } j \\ 0 & \text{otherwise} \end{cases} \qquad [23]$$

The digitalized image is then represented as:

$$\hat{f}(r,\phi) = \sum_{j=1}^{n} x_j \, b_j(r,\phi) \qquad [24]$$

Using a set of continuous functionals which assign to any picture f (r , ϕ) a real number $\mathcal{R}$ if, we can say that $\mathcal{R}$ if is the line integral of f (r , ϕ) along the i-th ray.

Then:

$$y_i \simeq \mathcal{R}_i f \simeq \mathcal{R}_i \hat{f} = \sum_{j=1}^{n} x_j \mathcal{R}_i b_j(r,\phi) = \sum_{j=1}^{n} x_j a_{ij} \qquad [25]$$

so we obtain a set of equations:

$$\mathbf{y} = A\mathbf{x} \qquad [26]$$

Unfortunately the number of pixel n and the number of rays m are in the order of 10^5 and the direct matrix inversion is not generally feasible.

One of the best known reconstruction technique is the Algebraic Reconstruction Technique (ART).

This is an iterative method where the image matrix $\mathbf{x}$ is initially assigned an arbitrary number. For each iteration the

matrix X is corrected (updated) by taking into account only a single ray and only the pixels intercepted by that ray. The discrepancy is redistributed along the pixels intercepted.

In formulas:

$$X^0 \in \mathbb{R}^m \qquad [27]$$

$$X^{k+1} = X^k + \frac{y_i - \langle a^i, x^k \rangle}{\|a^i\|^2} a^i \qquad [28]$$

where

$$\langle a^i, x^k \rangle = \sum_{j=1}^{m} a^i_j x^k_j \; ; \quad \|a^i\|^2 = \langle a^i, a^i \rangle ; \quad a^i = \left(a_{ij}\right)_{j=1}^{m}$$

The ART methods, and those derived from that, are very useful in image reconstruction as they are feasible for various projective geometries.

They can also be used in high contrast images, when the reconstruction can make use only of a few directions of view, or when execution time is crucial.

REFERENCES

The following references are quite complete reviews, giving a good perspective of reconstruction techniques and relating performances. The papers may be very useful for better comprehension of methods here presented in general terms.

[1] Bates R.H.T., Garden K.L., Peters T.M., "Overview of computerized tomography with emphasis on future developments", Proc. IEEE, vol. 71, pp. 356-372, March 1983.

[2] Lewitt R.M., "Reconstruction algorithms: Transform methods", Proc. IEEE, vol. 71, pp. 390-408, March 1983.

[3] Censor Y., "Fnite seriers-expansion reconstruction methods", Proc. IEEE, vol. 71, pp. 409-419, March 1983.